Experimental Investigation of the Signal Quality of One-way Scanning Laser Doppler Vibrometer on Different Materials

Shashanka Katta(✉), Yuanchen Zeng, and Zili Li

Department of Engineering Structures, Delft University of Technology, 2628 Delft, CN, The Netherlands
S.katta@tudelft.nl

Abstract. Vibrations of engineering structures can give insights into their dynamic properties and aid in assessing their health conditions and identifying damage. One-way scanning laser Doppler vibrometer (LDV) aims to scan structures along a certain path without stopping. The signal quality of one-way scanning LDV is affected by the surface characteristics of target structures. Different materials of engineering structures, such as steel, clay, and asphalt, exhibit different textures, roughness, and particle sizes. These differences can cause variations in backscattering and speckle patterns along the scanning path, affecting signal quality. This paper investigates how different materials and scanning speeds affect the signal quality of one-way scanning LDV through experiments. A rotating mirror directs the laser beam of an LDV to scan a vibrating beam with target surfaces made from clayey soil, sandy soil, steel, asphalt and wood at two different speeds: 0.6 ms^{-1} and 3 ms^{-1}. Subsequently, a two-step despeckling algorithm involving moving root mean square-based thresholding and an Empirical Mode Decomposition-based filter is applied to separate out the noise from the signal. The results indicate that noise power is much higher and signal-to-noise ratio (SNR) is significantly lower for clayey soil, sandy soil, and asphalt compared to wood and steel.

Keywords: Laser Doppler vibrometer · Speckle noise · Structural vibrations · Empirical Mode Decomposition · Noise power · Signal-to-noise ratio

1 Introduction

Vibrations provide valuable information on the dynamic properties of engineering structures and enable the characterization of their health [1,2]. Traditional contact sensors, such as accelerometers and geophones, are commonly used to measure structural vibrations. However, these sensors introduce additional mass

Á. Cunha and E. Caetano (Eds.): EVACES 2025, LNCE 674, pp. 105–115, 2025.
https://doi.org/10.1007/978-3-031-96110-6_8

to the target structure, potentially altering its dynamics. In the case of measuring the vibrations of large structures which are also slender, the contact sensor approach requires the installation of sensors at multiple locations, which can be time-consuming and labour-intensive, making it necessary to use non-contact based measurement approaches.

Laser Doppler Vibrometer (LDV) is a non-contact and non-destructive sensor for vibration measurement, with a broad frequency bandwidth. LDV operates by measuring the Doppler frequency shift in the backscattered laser beam from the target using the interferometry principle. The vibrational velocity of the target surface is thus decoded because it is proportional to the frequency shift.

LDVs can be used in different setups. These include single-point LDV, which measures the vibration at a single location; stepped scanning LDV, where measurements are taken sequentially across different points; continuous scanning LDV, in which repeated scanning is performed along a fixed loop [3]; and one-way scanning LDV (also referred to as LDV on moving platforms [4]), where the measurement is conducted continuously for a single time through an open path without retracing the previous path . One-way scanning LDV setups have been previously used to capture from moving vehicles the dynamic behaviour of long, slender structures such as rails [5] and roads [6].

The signal quality of the one-way scanning LDV is sensitive to the surface characteristics of target structures and the scanning speed. Different materials of engineering structures, such as steel, soil, and asphalt, exhibit different textures, roughness, and particle sizes. Such engineering surfaces can cause variations in signal dropouts due to different backscattering and also speckle patterns, due to the interference of dephased and coherent wavelets reflected from rough surfaces along the scanning path [3]. As the LDV scans such surfaces, the signal intensity and speckle patterns change drastically over time, leading to significant noise components in the LDV signal. Such noise typically manifests as dropouts or spikes in the time domain. The influence of the surface roughness of the structure being measured and scanning speed on speckle noise levels in one-way scanning LDV has been investigated. Experiments in [4] showed that, at higher scanning speeds, the spikes occur more frequently with larger amplitudes. Numerical simulations in [7] revealed that increasing surface roughness leads to a rise in speckle noise levels until saturation is reached. However, the previous research focused mainly on speckle noise but not on signal intensity variation, and the influence of surface roughness has not been studied experimentally.

Noise mitigation can be carried out in the measurement or post-processing stages [4]. In the measurement stage, it can be carried out, for example, by adjusting the sensitivity and focus of the laser spot [6]. In the post-processing stage, noise mitigation is challegning as speckle noise exhibits a broad range in the frequency spectrum, making it difficult to be mitigated using traditional band-pass filters, especially when the frequencies of interest of the vibration are broadband. Two-step despeckling algorithms have been proposed consisting of a detection step followed by an imputation or replacement step [4,5,8,9]. One of the approaches involves thresholding based on signal amplitude in the time domain, followed by Ensemble Empirical Mode Decomposition-based filtering. At a signal-to-noise ratio of -15dB, the Ensemble Empirical Mode Decomposition-based despeckling approach was shown to filter out noise more effectively than band-pass filtering and Discrete wavelet transform [5] especially when the frequency components of speckle noise overlaps with the vibrations. However, these existing despeckling methods have yet to be tested on structures made from different materials. In view of the research gaps, an experimental analysis is conducted in this study to investigate the variation in the signal quality of vibration measurements in one-way scanning setups. A two-step noise separation algorithm is employed to distinguish noise from vibration. The separated vibration and noise components are utilized to estimate the noise power level and signal-to-noise ratio of various target materials at two different scanning speeds.

The remainder of this paper is organised into four sections. Section 2 describes the experimental setup. Section 3 presents the signal processing methodology employed to separate noise from the vibration signal. Section 4 discusses the experimental results, and Sect. 5 summarizes the key findings and conclusions.

2 Experimental Setup

Figure 1 shows the schematic representation of the experimental setup. The laser beam from an RSV-150 LDV head was directed onto a cantilever beam using a rotating mirror, placed 4.46 m away from the cantilever beam. The cantilever beam, made from steel, has dimensions of 700 mm × 40 mm. The free end of the cantilever beam was subjected to a sinusoidal excitation using a shaker operating at a frequency of 200 Hz. Various material samples, including wood (460 mm × 60 mm), asphalt (160 mm × 38 mm), clayey soil (660 mm × 35 mm), and sandy soil (660 mm × 35 mm), were individually affixed to the cantilever beam using magnets, as shown on Fig. 2. The laser beam scanned along a straight line across the cantilever beam (with or without the attached samples). The rotational speed of the mirror was adjusted to scan at speeds of 0.6 ms^{-1} and 3 ms^{-1}. The LDV measurements were recorded using PAK MK II 5.8 system and sampled at 51.2 kHz.

3 Signal Processing Methodology

The vibrations of the different target material samples are measured using the LDV setup. Figure 3 shows the vibration of a steel beam. The measured signals contain noise appearing as spikes. These spikes distort the signal waveform. A noise separation algorithm, inspired by [10] has been implemented. Subsequently, the noise power and SNR are calculated for the vibrations corresponding to different materials.

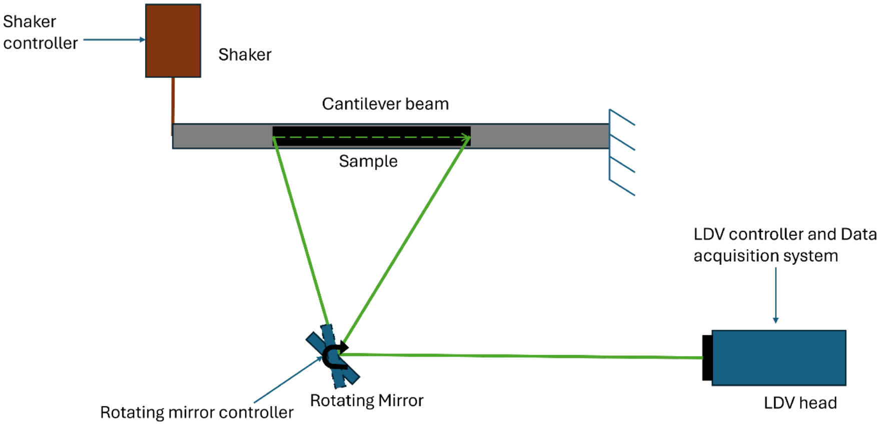

Fig. 1. Schematic diagram of the experimental setup

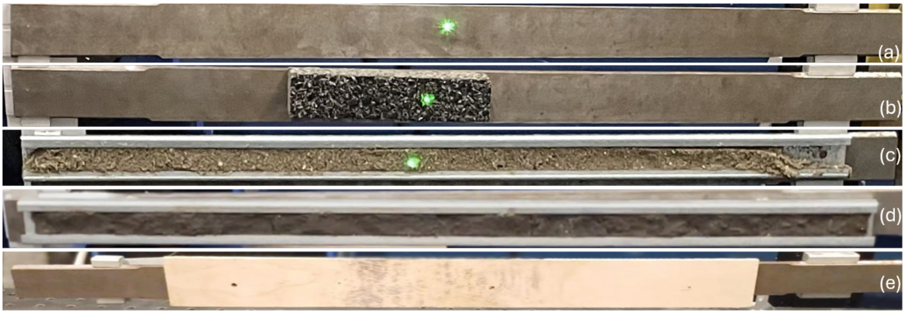

Fig. 2. Target materials affixed on the cantilever beam: a) Steel b) Asphalt c) Sandy soil d) Clayey soil e) Wood

3.1 Noise-Separation Algorithm

Large spikes exhibit broad frequency contents and can distort the signal even after filtering due to the presence of low-frequency components. To mitigate the effect of spikes, a moving root mean square (RMS) threshold is applied to truncate spikes that exceed the threshold limits. The signal is divided into non-overlapping segments of a defined length. In each segment, signal values exceeding the threshold values for the segment, are replaced by the respective threshold values. The thresholds for each signal segment are determined by Eq. 1. In this formulation, $S_u(t)$ and $S_l(t)$ are the upper and lower threshold, $S(t)$ is the measured velocity at time instant t in the signal, N is the length of the segment and $\bar{v}(t)$ is the average of the signal segment values. The measured signal is thus, decomposed into $S_T(t)$, the signal after thresholding and noise as shown in Eq. 2.

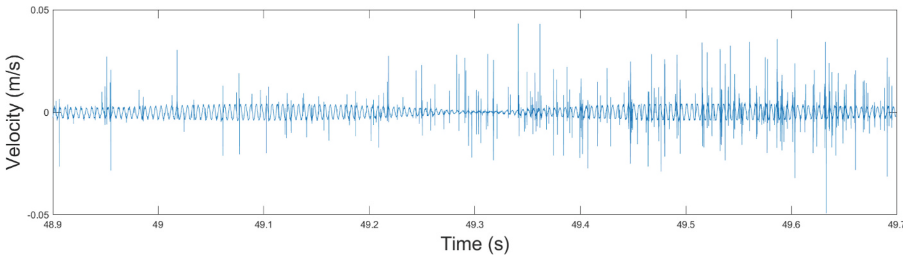

Fig. 3. Vibrations of steel beam measured using LDV at a scanning speed of 0.6 ms^{-1}

$$S_u(t) = \bar{v}(t) + 2\sqrt{\frac{\sum_{t=0}^{N}(v(t)-\bar{v}(t))^2}{N}}$$
$$S_l(t) = \bar{v}(t) - 2\sqrt{\frac{\sum_{t=0}^{N}(v(t)-\bar{v}(t))^2}{N}} \tag{1}$$

$$S(t) = S_T(t) + \text{Noise} \tag{2}$$

The signal after thresholding is subsequently denoised using the EMD algorithm, introduced by Huang et al. [11]. The algorithm decomposes signals into a series of components termed Intrinsic Mode Functions (IMFs) and a residual signal. IMFs provide information about the instantaneous frequency and represent local modal responses. The lower-order IMFs capture high-frequency behaviour, which, in this paper, corresponds mainly to noise and is separated from the rest of the signal to obtain the vibrational content. Equation 3 shows the signal after thresholding, represented as $S_T(t)$ with it's IMFs and a residual. The first K modes in the signal represent the noise, with the remaining modes and residual representing the vibration component. To mitigate mode mixing, Ensemble Empirical Mode Decomposition (EEMD) has been suggested by Jin et al. [5]. However, EMD and EEMD produced similar results for the denoised signals examined in this study. Consequently, EMD was selected to reduce computational time and obtain the variation of noise over time.

$$\begin{aligned} S_T(t) &= \sum_{i=1}^{M} \mathrm{IMF}_i + \text{residual} \\ &= \underbrace{\sum_{i=1}^{K-1} \mathrm{IMF}_i}_{\text{Noise}} + \underbrace{\sum_{i=K}^{M} \mathrm{IMF}_i + \text{residual}}_{\text{Vibration}}. \end{aligned} \tag{3}$$

By combining Eqs. 2 and 3, noise signal is obtained by summing up noise separated in the two steps.

3.2 Quantification of Noise

The noise level in the measurements is calculated using noise power and signal-to-noise ratio (SNR) for each noise signal. Noise Power is defined as the RMS of the noise signal, while signal power as the RMS of the vibration signal. The SNR is obtained by dividing the signal power by the noise power and provides the noise level relative to the signal. In this paper, the variations of both noise power and SNR will be discussed.

4 Results

4.1 Noise Separation Algorithm

Noise is estimated through the two-step process. In the RMS thresholding of the signal, the parameter N is set to 1000. Figure 4 illustrates the boundaries for a one-second sample of vibration data collected from a steel specimen at a scanning speed of 0.6 ms^{-1}.

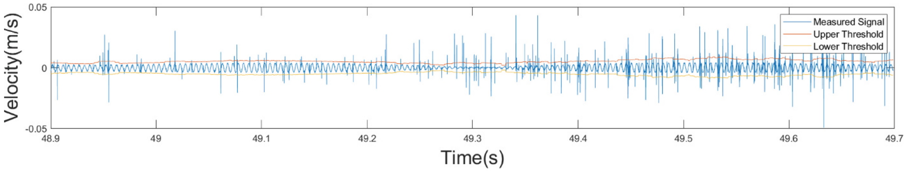

Fig. 4. Moving root mean square threshold

In the second stage, EMD-based noise separation is performed by identifying and distinguishing IMFs associated with noise to extract the vibration signal. Figure 5 presents the first two IMFs (K=2), which exhibit significant spikes and are consequently removed. This procedure is repeated for signals corresponding to different target materials and scanning speeds. The parameters remained the same across all cases.

Figure 6 presents the raw and noise separated one-second vibration signals recorded during the scanning of various material samples at a speed of 0.6^{-1}. The time-history plots indicate that forced vibrations at 200 Hz were successfully captured in the vibration signals. Noise appearing in the form of spikes occurs more frequently in clayey soil, asphalt, and sandy soil samples, with the spike amplitudes being significantly larger in clayey soil, asphalt and sand compared to other materials. Minor distortions remain in the vibration signals for the clayey soil, asphalt, and sand samples. Furthermore, at locations with intense speckle noise, residual noise is still present in the processed vibration signals. However, they are significantly smaller in amplitude in comparison to the noise level before noise separation.

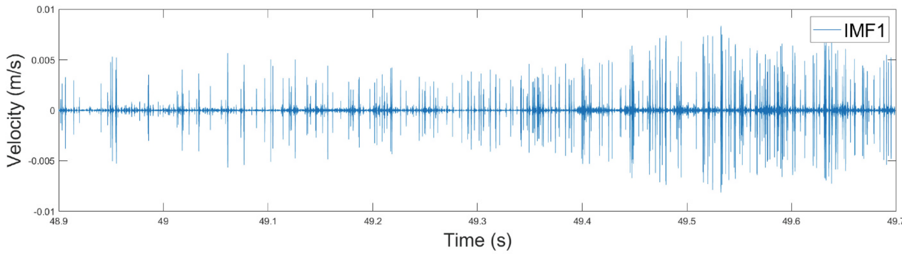

(a) First IMF

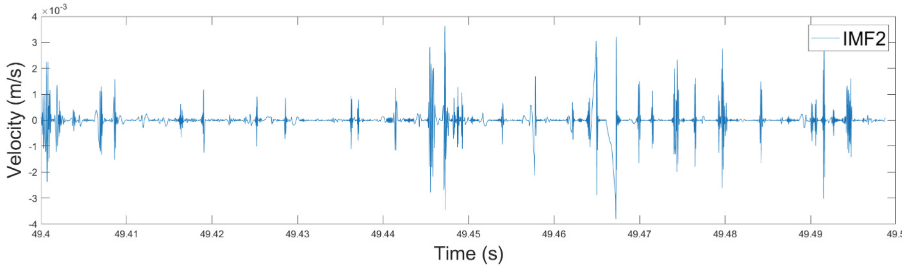

(b) Second IMF

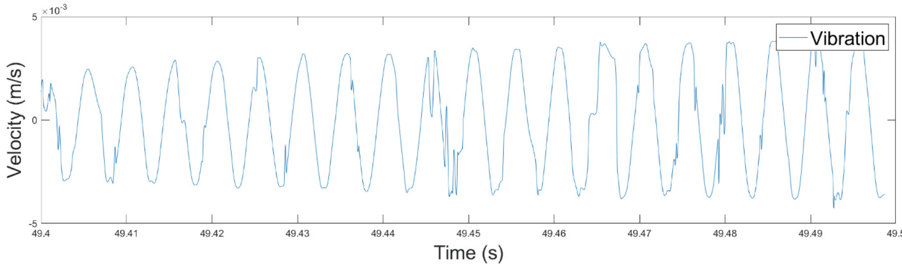

(c) Vibration component of the signal

Fig. 5. The first two IMFs and vibration component of steel captured while scanning at 0.6 ms^{-1}

4.2 Noise Power and SNR for Different Materials at Two Scanning Speeds

s Figures 7 and 8 illustrate the variation in noise power and SNR for the tested material samples across the two scanning speeds. The noise level is much lower and the signal quality is notably higher from steel and wood surfaces than from the clayey soil, asphalt, and sand samples. The wood and steel surfaces tested were smooth with relatively low surface roughness, resulting in much lower noise levels in the measured signals. Even though the noise power is similar for both wood and steel samples, the SNR of wood is higher than steel. This is due to the vibration amplitude being larger for the wood sample. It can also be noted that across all materials, noise power and SNR remained roughly similar across different scanning speeds. In contrast to the wood and steel samples, the asphalt surface, as shown in Fig. 2, contains numerous pores where light can be trapped, potentially leading to poor backscattering. Changes in surface texture along the scanning path of clayey soil and sandy soil and the movement of loose sand particles during vibration may have contributed to the reduced SNR of clayey soil and sandy soil. Surface irregularities caused by the presence of vegetation may have further exacerbated the low signal-to-noise ratio of clay samples. Noise

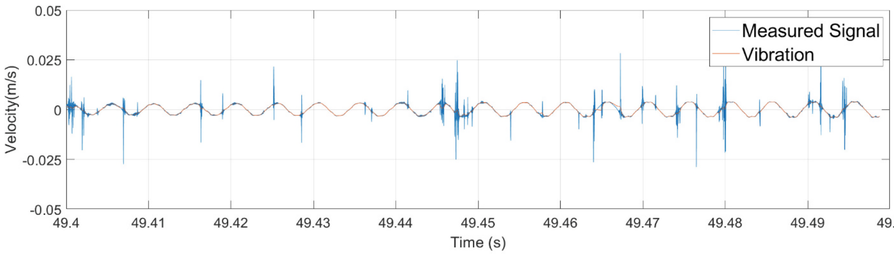

(a) Steel

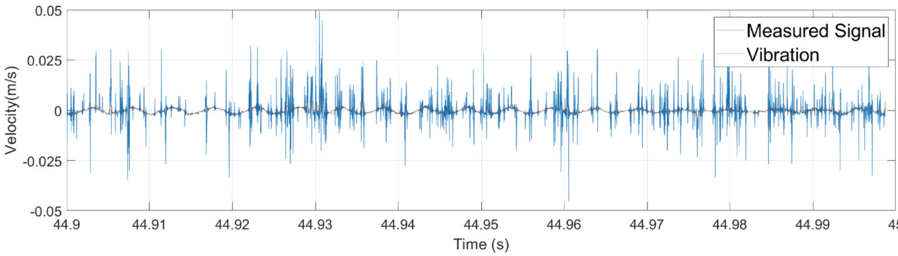

(b) Clay

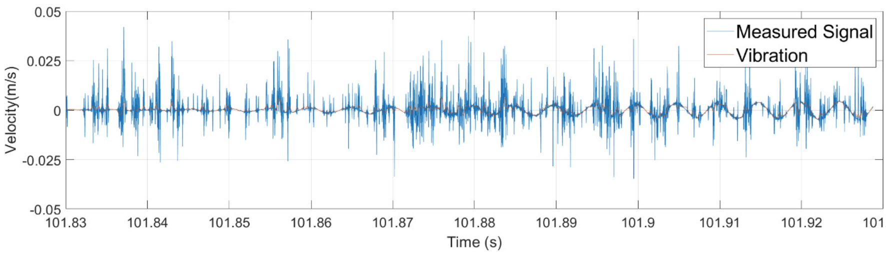

(c) Asphalt

Fig. 6. Target vibrations of different materials measured at a scanning speed of 0.6 ms^{-1}

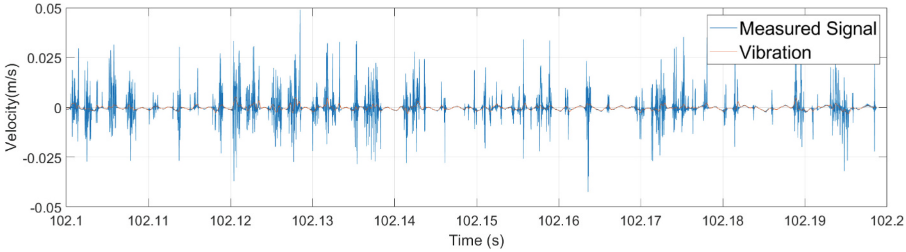

(d) Sand

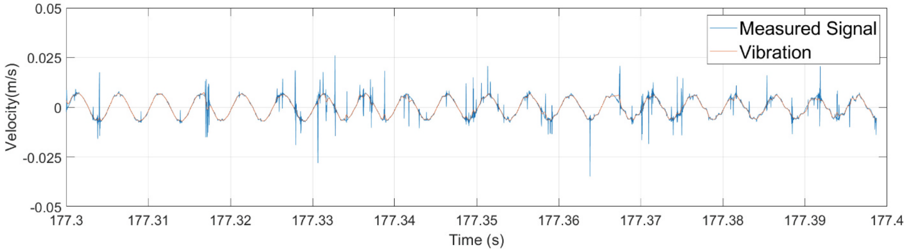

(e) Wood

Fig. 6. (*continued*)

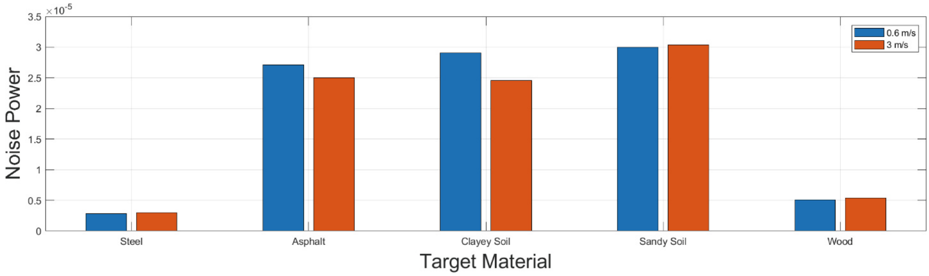

Fig. 7. Comparison of noise power across materials and speeds

power and SNR do not exhibit substantial variation with changes in scanning speed for all material samples. This contrasts with earlier studies suggesting a positive correlation between scanning speed and speckle noise power.

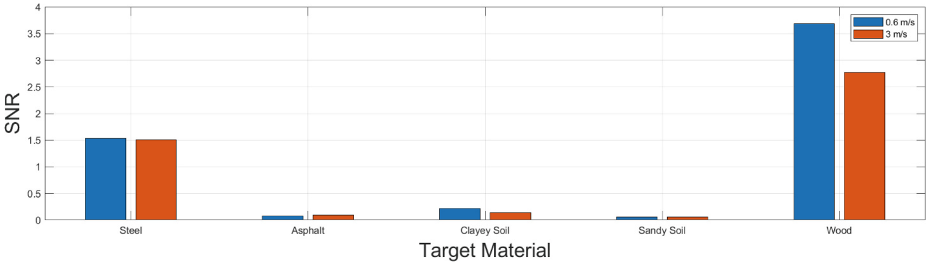

Fig. 8. Comparison of SNR across materials and speeds

5 Conclusions

This paper investigates the variation of noise power and signal-to-noise ratio while scanning different target materials using one-way scanning LDV. The main takeaways are presented below:

1. EMD-based noise separation algorithm effectively reduces speckle noise across all material samples. Minor distortions remain but do not significantly affect noise power and signal-to-noise quality.
2. Materials like steel and wood, with smooth surfaces, produce lower noise power and higher SNR compared to clayey soil, asphalt, and sandy soil. In the case of the latter three, surface roughness, presence of surface pores, and weakly-bound surface particles may lead to poor backscattering leading to higher noise power and lower SNR in the signals.

Future studies may be carried out by varying individual properties for each material to adjudge the main factors affecting the signal quality as well as to understand the speckle noise behaviour across different scanning speeds.

Acknowledgement. This research was supported by ProRail under the RESET (Reliable Embankments for Safe Expansion in Rail Traffic) Project.

References

1. Carden EP, Fanning P (2004) Vibration Based Condition Monitoring: A Review. In: Structural Health Monitoring, vol 3, no 4, pp 355–377
2. Jones R (1962) Surface wave technique for measuring the elastic properties and thickness of roads: Theoretical Development. In: British Journal of Applied Physics, vol 13, no 1, pp 21–29
3. Rothberg S et al (2017) An international review of laser Doppler vibrometry: Making light work of vibration measurement. Optics Lasers Eng 99:11–22
4. Zeng Y, Núñez A, Li Z (2022) Speckle noise reduction for structural vibration measurement with laser Doppler vibrometer on moving platform. In: Mechanical Systems and Signal Processing, vol 99, pp: 11–22

5. Jin Y, Dollevoet R, Li Z (2022) Removing speckle noise from the signals of a laser Doppler vibrometer on moving platforms (LDVom) by ensemble empirical mode decomposition. In: Measurement Science and Technology, vol 33, no 12, p 125205
6. Jiang LA, et al (2011) Laser vibrometry from a moving ground vehicle. In: Applied Optics, vol 50, no 15, p 2263
7. Jin Y, Dollevoet R, Li Z (2022) Numerical simulation and characterization of speckle noise for laser Doppler vibrometer on moving platforms (LDVom). In: Optics and Lasers in Engineering, vol 158, p 107135
8. Kaynardag K, Yang C, Salamone S (2025) An impulsive noise filter for rail vibration measurements using a laser Doppler vibrometer on a moving platform. In: Mechanical Systems and Signal Processing, vol 223, p 111918
9. Kaynardag K, Yang C, Salamone S (2023) A rail defect detection system based on laser Doppler vibrometer measurements. In: NDT & E International, vol 137, p 102858
10. Jin Y, Li Z (2021) A new method for eliminating speckle noise from Laser Doppler Vibrometer signals. In: Journal of Physics: Conference Series, vol 2041, p 012007
11. Huang NE, et al (1998) The empirical mode decomposition and the Hilbert spectrum for nonlinear and non-stationary time series analysis. In: Proceedings of the Royal Society of London. Series A: Mathematical, Physical and Engineering Sciences, vol 454, no 1971, pp 903–995